Moment capacity of beam-to-column minor-axis joints

Autor(en): **Gomes, Fernando / Jaspart, Jean-Pierre / Maquoi, René**

Objekttyp: **Article**

Zeitschrift: **IABSE reports = Rapports AIPC = IVBH Berichte**

Band (Jahr): **75 (1996)**

PDF erstellt am: **13.07.2024**

Persistenter Link: https://doi.org/10.5169/seals-56922

Nutzungsbedingungen

Die ETH-Bibliothek ist Anbieterin der digitalisierten Zeitschriften. Sie besitzt keine Urheberrechte an den Inhalten der Zeitschriften. Die Rechte liegen in der Regel bei den Herausgebern.
Die auf der Plattform e-periodica veröffentlichten Dokumente stehen für nicht-kommerzielle Zwecke in Lehre und Forschung sowie für die private Nutzung frei zur Verfügung. Einzelne Dateien oder Ausdrucke aus diesem Angebot können zusammen mit diesen Nutzungsbedingungen und den korrekten Herkunftsbezeichnungen weitergegeben werden.
Das Veröffentlichen von Bildern in Print- und Online-Publikationen ist nur mit vorheriger Genehmigung der Rechteinhaber erlaubt. Die systematische Speicherung von Teilen des elektronischen Angebots auf anderen Servern bedarf ebenfalls des schriftlichen Einverständnisses der Rechteinhaber.

Haftungsausschluss

Alle Angaben erfolgen ohne Gewähr für Vollständigkeit oder Richtigkeit. Es wird keine Haftung übernommen für Schäden durch die Verwendung von Informationen aus diesem Online-Angebot oder durch das Fehlen von Informationen. Dies gilt auch für Inhalte Dritter, die über dieses Angebot zugänglich sind.

Ein Dienst der *ETH-Bibliothek*
ETH Zürich, Rämistrasse 101, 8092 Zürich, Schweiz, www.library.ethz.ch

http://www.e-periodica.ch

Moment capacity of beam-to-column minor-axis joints

Fernando GOMES
Assistant
Dep. of Civil Eng.
University of Coimbra
Portugal

Jean-Pierre JASPART
Associate Researcher
Dep. MSM
University of Liège
Belgium

René MAQUOI
Professor
Dep. MSM
University of Liège
Belgium

Summary

This paper presents a method of prediction the moment capacity of beam-to-column minor-axis joints, where the beam is directly connected to the web of an I section column, causing bending about the minor-axis of the column section. The strength is limited by the formation of plastic failure mechanisms in the column web. Several failure modes for bolted and welded connections are discussed, and a design method based on yield line theory is proposed. The method is also applicable to the design of connections between a beam and a RHS column.

1. Introduction

Fig. 1 shows some common types of beam-to-column minor-axis joints where the beam is directly connected to the column web without stiffeners. The connection can be welded or bolted using web cleats, flange cleats, flush end plates or extended end plates.

The revised Annex J [1] of the Eurocode 3 provides design rules for the evaluation of the resistance of connecting elements (end plates, cleats, bolts) but it does not cover the common case of failure due to the out-of-plane deformation of the column web.

Failure mechanisms of the column web are briefly described in this paper and it should be emphasised that the same kind of mechanisms can be observed in the case of connections between a beam and a rectangular hollow section (RHS) column, Fig. 2. These failure mechanisms are divided into two main groups: *Local* and *Global* mechanisms, described hereafter. A local failure means that the yield line pattern is localised only in the compression zone or in the tension zone, Fig. 3, while in the global failure the yield line pattern involves both compression and tension zones, Fig. 4.

The moment transmitted by the beam to the column web may be decomposed in a couple of forces F acting in the compression and tension zones. Two different loading cases are analysed:

— *Loading case* 1: the load F acts on a rigid rectangle with the dimensions $b \times c$, Fig. 5, as in the case of a welded connection where these dimensions are defined by the perimeter of the welds around the beam flange;
— *Loading case* 2: the load F is transmitted by one or more rows of bolts, as in the tension zone of the bolted connections represented in Fig. 6 and 8.

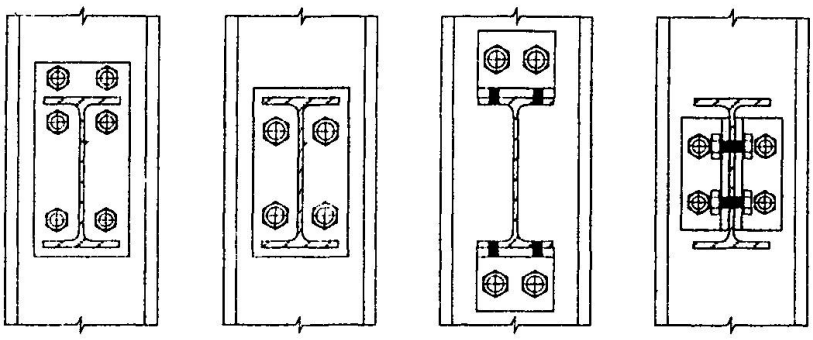

a) extended end plate *b) flush end plate* *c) flange cleats* *d) web cleats*

Fig. 1. Beam-to-I section column minor-axis joints

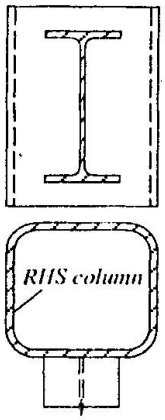

Fig. 2. Beam-to-RHS column joint

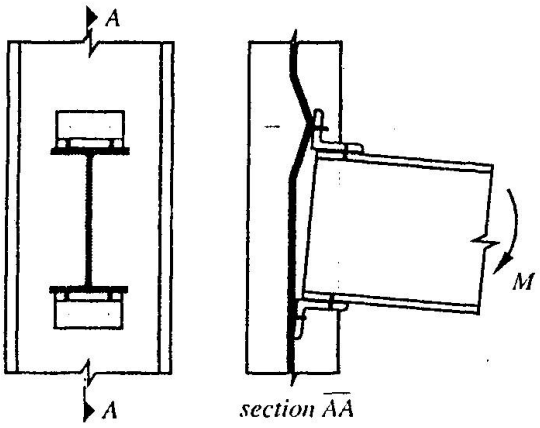

Fig. 3. Local mechanism

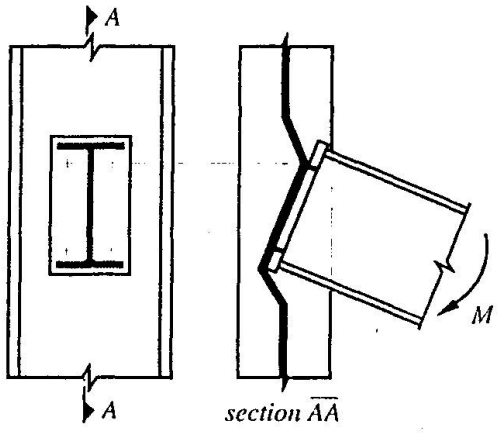

Fig. 4. Global mechanism

2. Local failure

2.1 Flexural mechanisms

Basic failure mechanisms are obtained by the Johansen yield line method, using log-spiral fans in order to optimise the yield line pattern. The plastic moment per unit length of yield line is given by

$$m_{pl} = 0{,}25\ t_w^2 f_y \qquad (1)$$

(f_y = yield stress; t_w = thickness of the column web).

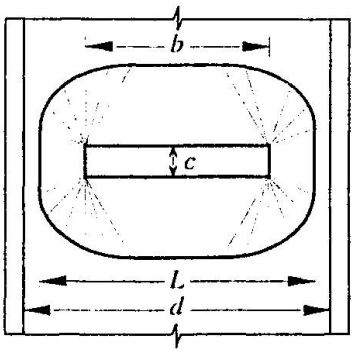

Fig. 5. Yield line pattern (Local mechanism)

In the flexural mechanisms, it is assumed that the plastic moment is not reduced by the presence of shear force perpendicular to the plane of the web; this reduction is taken into account in section 2.3. The plastic failure load associated to the optimised mechanism of Fig. 5, for F acting on a rectangle $b \times c$ (*loading case* 1), is given by

$$F_{pl} = 4\pi m_{pl}\left(1+\frac{4}{\pi}\cot\theta+\cot^2\theta+\frac{2c}{\pi(L-b)}\right),$$

where θ is the solution of the equation $\dfrac{b}{L-b} = 2\,e^{\frac{\pi}{2}\cot\theta}\cot\theta$, and $L = d - 1{,}5r$.

For practical design purposes it is desirable to make use of a simplified formula, explicit in F_{pl}, which may be given by the approximate solution

$$F_{pl} = \frac{4\pi m_{pl}}{1-\dfrac{b}{L}}\left(\sqrt{1-\frac{b}{L}} + \frac{2c}{\pi L}\right). \qquad (2)$$

For the *loading case* 2 (e.g. Fig. 6), the mean diameter of the bolt head, Fig. 7, is defined by

$$d_m = \frac{d_1 + d_2}{2}. \qquad (3)$$

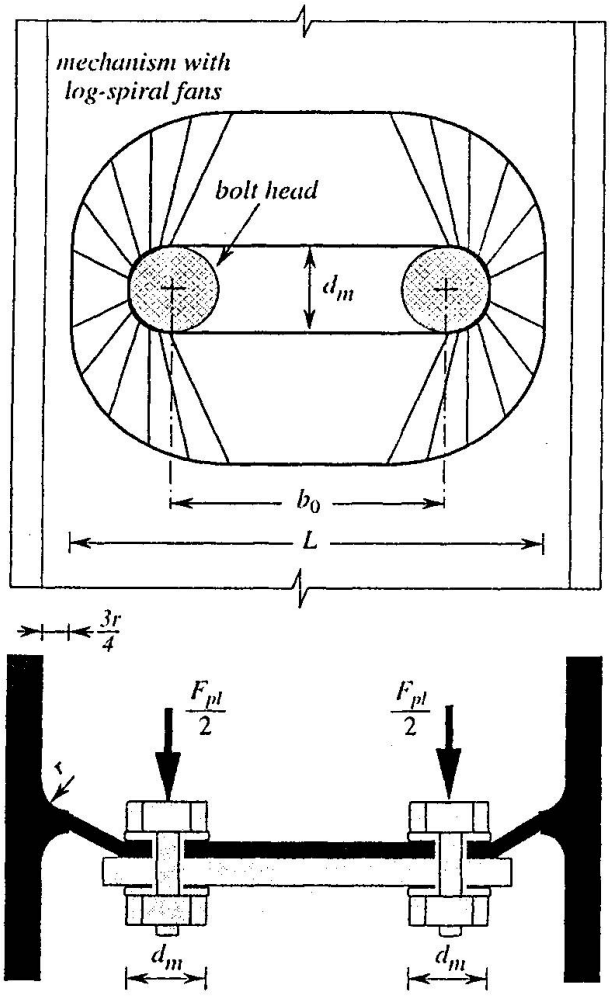

Fig. 6. Failure mechanism of bolted connection

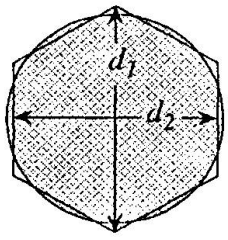

Fig. 7. Bolt head (or nut)

The yield line mechanism of Fig. 6 leads to the plastic load

$$F_{pl} = \frac{4\pi m_{pl}}{1-\dfrac{a^*}{L-b_1}}\left(1 + \frac{4}{\pi}\cot\theta + \cot^2\theta\right),$$

where $a^* = d_m\, e^{-\frac{\pi}{2}\cot\theta}$,

$$b_1 = b_0 + d_m\left(1 - e^{-\frac{\pi}{2}\cot\theta}\right),$$

and θ is the solution of the equation

$$\frac{b_1}{L-b_1} = 2e^{\frac{\pi}{2}\cot\theta}\cot\theta\,.$$

Instead of this complex system of equations, the simplified formula (2) may also be used for the evaluation of the failure load in the tension zone, Fig. 8, if this zone is replaced by an equivalent rectangle with the dimensions:

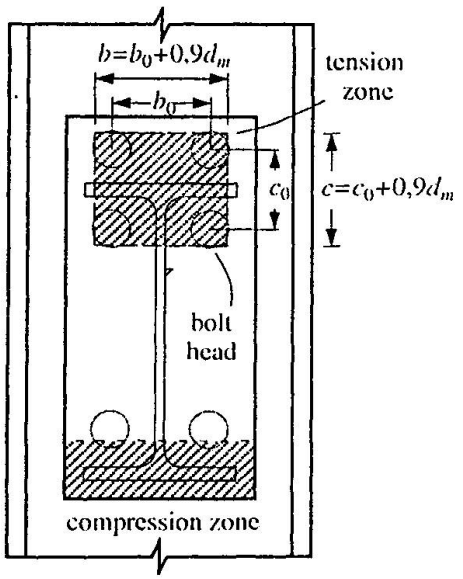

Fig. 8. Bolted connection

$$\begin{cases} b = b_0 + 0{,}9 d_m \\ c = c_0 + 0{,}9 d_m \end{cases} . \tag{4}$$

The same formula (2) may therefore be used in the two loading cases.

2.2 Punching shear mechanisms

For the *loading case* 1 the punching perimeter is a rectangle with the dimensions $b \times c$. The punching load is then given by

$$F_{punch} = 2(b+c)\, v_{pl}, \quad \text{where } v_{pl} = t_w f_y / \sqrt{3}. \tag{5}$$

For the *loading case* 2 the punching of the column web around each bolt head must be checked. If there are n bolts in the tension zone, the punching load is given by

$$F_{punch} = n \pi d_m v_{pl}. \tag{6}$$

2.3 Combined flexural and punching shear mechanisms

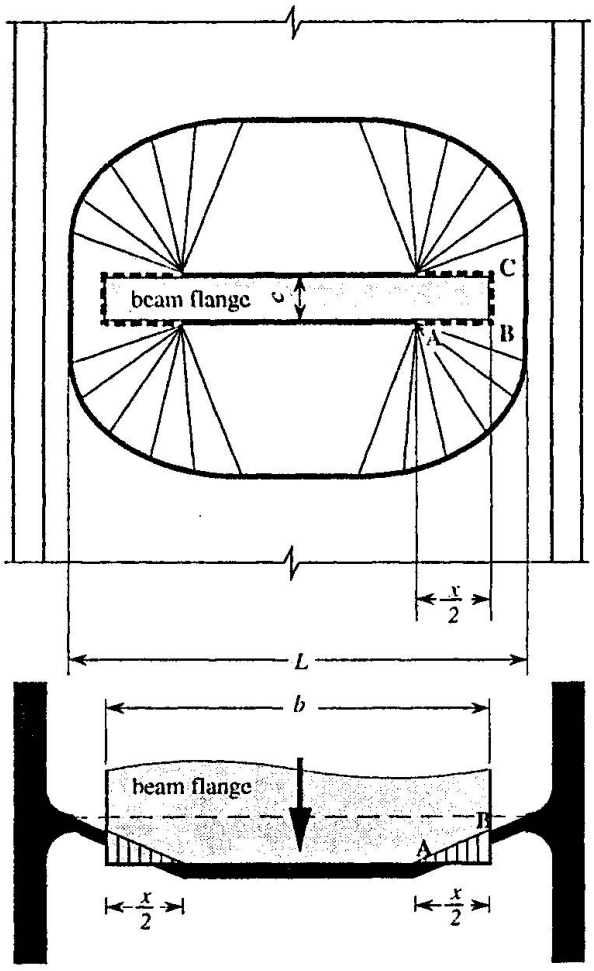

Fig. 9. Combined flexural and punching shear failure

A combined flexural and punching shear mechanism presents not only flexural yield lines (thick lines in Fig. 9) but also punching shear yield lines (dotted lines in Fig. 9). Packer *et al* [2] proposed similar combined failure modes using straight lines or circular fans, instead of the optimised mechanism of Fig. 9 that uses log-spiral fans.

The present solution also takes into account that the plastic moment per unit length of yield line is reduced by the presence of shear when v (the shear force per unit length)

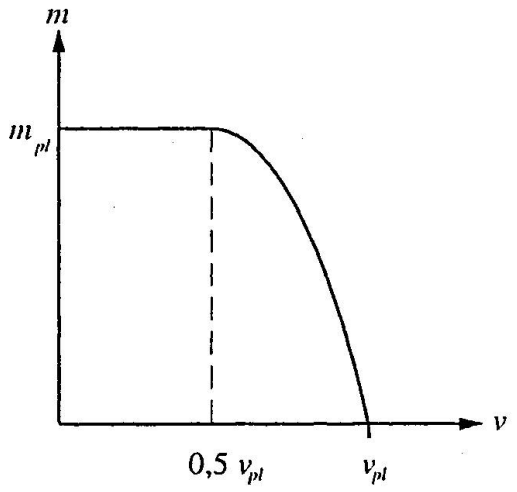

Fig. 10. Interaction between m (moment) and v (shear force)

exceeds 50% of v_{pl}, according to the interaction diagram of Fig. 10. This provides a refinement of the previous solution proposed by the authors [3]. In spite of the refinement, the expression for the plastic load is presented in a simpler form (avoiding the iterative procedure of the previous solution):

$$F_{Q2} = 4\, m_{pl}\left[\frac{\pi\sqrt{L(a+x)}+2c}{a+x} + \frac{1{,}5\,c\,x+x^2}{\sqrt{3}\,t_w\,(a+x)}\right], \tag{7}$$

where: $a = L-b$,

$$\begin{cases} x=0 & \text{if } b \le b_m \\ x=-a+\sqrt{a^2-1{,}5\,ac+\dfrac{\sqrt{3}\,t_w}{2}\left[\pi\sqrt{L\,(a+x_0)}+4c\right]} & \text{if } b \ge b_m \end{cases},$$

$$x_0 = L\left[\left(\frac{t}{L}\right)^{\frac{2}{3}} + 0{,}23\frac{c}{L}\left(\frac{t}{L}\right)^{\frac{1}{3}}\right]\left(\frac{b-b_m}{L-b_m}\right)$$

and $$b_m = L\left[1-0{,}82\frac{t_w^2}{c^2}\left(1+\sqrt{1+2{,}8\frac{c^2}{t_w L}}\right)^2\right], \quad \text{but } b_m \ge 0, \tag{8}$$

Equation (7) provides an additional advantage with respect to the pervious solution [3]: it may be applied in the full range $0 \le b \le L$, instead of the previous constraint $b \le 0{,}8L$.

For the *loading case* 2 (bolted connections) the equivalent rectangle, defined by equation (4), may be used.

2.4 Correction to take into account the difference between Johansen and Von Mises yield criteria

The plastic failure loads obtained by the yield line method differ from the exact solutions based on the Von Mises yield criterion. It was shown [5] that if $(b+c)/L \ge 0{,}5$ the optimised yield line mechanisms provide an accurate solution. However, if $(b+c)/L < 0{,}5$, the yield line method overestimates the plastic load. The influence of the yield criteria on the plastic load was evaluated by numerical simulations performed with the finite element program FINELG [4] that uses the Von Mises yield criterion, instead of the square yield criterion (Fig. 11) used in the Johansen yield line method.

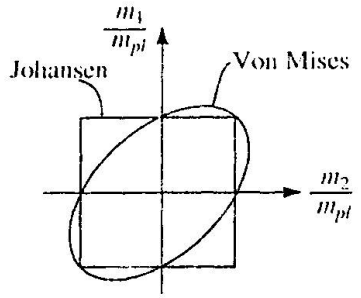

Fig. 11. Yield criteria for plates (m_1, m_2 - principal moments)

Final expressions for flexural mechanism as well as for combined mechanism should then include a correction factor k that multiplies Eq. (2) or Eq.(7) in order to obtain an accurate plastic load. The correction factor k may be evaluated as [5]:

$$k = \begin{cases} 1 & \text{if } (b+c)/L \ge 0{,}5 \\ 0{,}7+0{,}6(b+c)/L & \text{if } (b+c)/L \le 0{,}5 \end{cases}. \tag{9}$$

2.5 Comparison between the three modes of local failure

It is obvious that equations (7) and (2) are identical when $x = 0$ (no punching), meaning that the combined mechanism is transformed into the pure flexural mechanism. This occurs when $b \le b_m$, where b_m is the particular value of b that determines the boundary between the two mechanisms. When $b > b_m$ equation (7) gives a plastic load always smaller than equation (2), which means that equation (2) is useless.

The local failure mechanism is the mechanism associated to the lowest plastic load which is then given by

$$F_{local} = \min\left(F_{punch}; k F_{Q2}\right). \tag{10}$$

The three modes of local failure are compared in Fig. 12 for a bolted connection with two bolts in the tension zone, like that of Fig. 6. The bolted diameter is fixed to $d_m = 0{,}1\,L$, and from equation (4) the equivalent rectangle is defined by $b = b_0 + 0{,}09\,L$ and $c = 0{,}09\,L$. Fig. 12 shows the variation of the failure load (thick line) as a function of b, representing the three modes of failure.

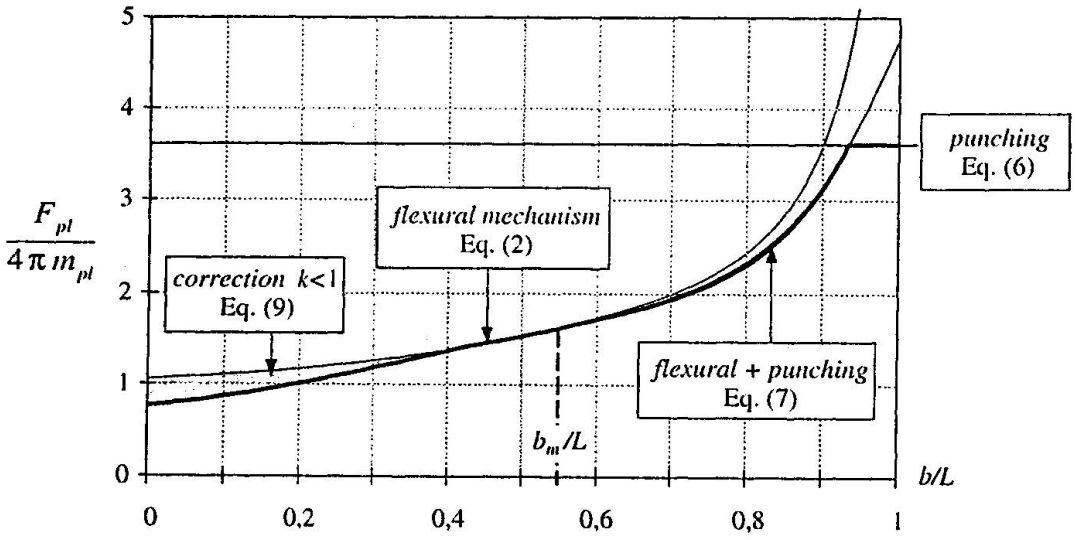

Fig. 12. Comparison between the three modes of local failure

3. Global failure

The global failure load, for flexural mechanisms or for combined flexural and punching mechanisms, may be evaluated as

$$F_{global} = \frac{k F_{Q2}}{2} + m_{pl}\left(\frac{2b}{h} + \pi + 2\rho\right), \tag{11}$$

where F_{Q2} and k are given by equations (7) and (9), h is the distance between centres of compression and tension zones, and ρ is given by

$$\begin{cases} \rho = 1 & \text{if } 0,7 \le \dfrac{h}{L-b} \le 1 \\ \rho = \dfrac{h}{L-b} & \text{if } 1 \le \dfrac{h}{L-b} \le 10 \end{cases}$$

Outside the range $0,7 \le \dfrac{h}{L-b} \le 1$ equation (11) is no more valid. However it underestimates the plastic load if the following values of ρ are assumed:

$$\begin{cases} \rho = 1 & \text{for } \dfrac{h}{L-b} < 0,7 \\ \rho = 10 & \text{for } \dfrac{h}{L-b} > 10 \end{cases}$$

Global failure mechanisms involve both compression and tension zones, Fig. 4. These mechanisms are assumed to be symmetrical with respect to a horizontal and to a vertical axis in the plane of the column web. The horizontal symmetry is not an exact assumption when the dimensions $b \times c$ of the compression zone are different from those of the tension zone, e.g. Fig. 8. In this case equation (11) should be applied separately for each zone, leading to two different loads, and the failure load will be an intermediate value. However the two zones are often assumed to be equal (see section 4) and then equation (11) will be applied only once.

4. Ultimate moment

The ultimate moment is finally obtained by $M_{pl} = h \times \min\left(F_{local}, F_{global}\right)$ where h is the distance between centres of compression and tension zones. It may be assumed, in common cases, that the beam only transmits moment to the column (no axial force in the beam) which means that the compression and tension forces are equal. Referring to the connection in Fig. 8, the tension force is first evaluated and, as the compression force is equal to the tension force, the dimension c of the compression zone will be determined in order to have the same plastic load. As an alternative to this determination of h, a direct evaluation of this value may be obtained by assuming that compression and tension zones have the same dimensions $b \times c$.

In some situations (e.g. Fig. 13), h_t and b are known, but c is indeterminate. From the condition of moment maximisation with respect to c, the following c may be obtained:

$$c = h_t\left(0,3\frac{b}{L} + 0,1\frac{h_t}{L} - 0,15\right) \quad \text{but} \quad 0 < c < 0,5h_t.$$

5. Conclusions

The evaluation of the moment capacity of minor-axis joints is a complex task due to the large number of failure modes of the column web. The proposed method, however, predicts these failure modes with few expressions, easy to use by designers. Comparisons of theoretical predictions with 12 experimental tests [6] and with a large number of numerical simulations [7] confirm the accuracy of the analytical method. Details on the background of this method may be found in [8].

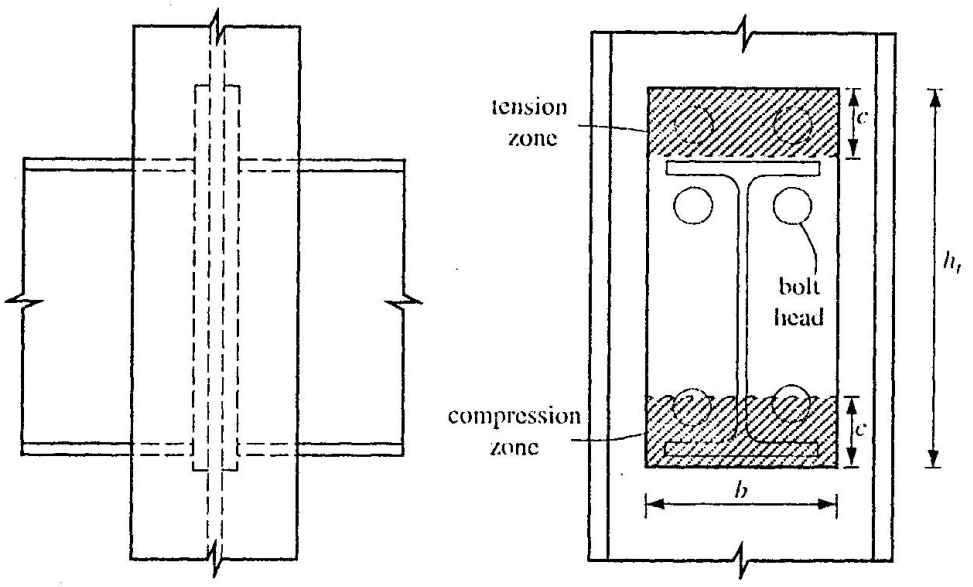

a) side view *b) front view*

Fig. 13. Joint with two beams one of each side of the column web

References

[1] Eurocode 3 - *Design of steel structures* , part 1-1, General rules and rules for buildings, CEN, ENV 1993-1-1, 1992, Including Revised Annex J - *Joints in building frames*, 1994.

[2] Packer, J. A., Morris, G. A. and Davies, G. - *A Limit state design method for welded tension connections to I-sections webs*, J. of Constructional Steel Research, Vol. 92, 1989, pp. 33-53.

[3] Gomes, F. C. T, Jaspart, J.-P., Maquoi, R. - *Behaviour of minor-axis joints and 3-D joints*, Proceedings of the Second State of the Art Workshop COST C1 on Semi-rigid Connections, Ed.: F. Wald, Czech Technical University, Prague, 26 - 28.10.1994. pp. 111-120.

[4] Frey, F., De Ville de Goyet V., *et al.* - *FINELG - Non-linear Finite Element Analysis Program - User's Manual Version 5.2*, University of Liège, March, 1990.

[5] Gomes, F. C. T. - *État limite ultime de la résistance de l'âme d'une colonne dans un assemblage semi-rigide d'axe faible*, Internal Report N°. 203, Dept. MSM, University of Liège, 1990.

[6] Gomes, F.C.T., Jaspart, J.-P. - *Experimental research of minor-axis joints. Comparison with theoretical predictions*, COST C1 - WG2 "Steel and Composite" Meeting, Doc. C1/WD2/94-13, Coimbra, 25 - 26.11.1994.

[7] Neves, L.F.C., Gomes, F.C.T. - *Semi-rigid behaviour of beam-to-column minor-axis joints*, IABSE Colloquium, Istanbul, 25 - 27.09.1996.

[8] Gomes, F. C. T. - *Comportement semi-rigide de nœuds poutre-colonne d'axe faible et résistance de nœuds tridimensionnels en acier*, Doctoral thesis (to be submitted at the University of Liège).